Enhanced in vitro biocompatibility of ultrafine-grained titanium with hierarchical porous surface

C.Y. Zheng [a,b], F.L. Nie [a,b], Y.F. Zheng [a,b,*], Y. Cheng [b], S.C. Wei [c,**], R.Z. Valiev [d]

[a] State Key Laboratory for Turbulence and Complex System and Department of Advanced Materials and Nanotechnology, College of Engineering, Peking University, Beijing 100871, China
[b] Center for Biomedical Materials and Tissue Engineering, Academy for Advanced Interdisciplinary Studies, Peking University, Beijing 100083, China
[c] Department of Oral and Maxillofacial Surgery, School of Stomatology, Peking University, Beijing 100081, China
[d] Institute of Physics of Advanced Materials, Ufa State Aviation Technical University, Ufa, Russia

ARTICLE INFO

ABSTRACT

Bulk ultrafine-grained Ti (UFG Ti) was successfully fabricated by equal-channel angular pressing (ECAP) technique in the present study, and to further improve its surface biocompatibility, surface modification techniques including sandblasting, acid etching and alkali treatment were employed to produce a hierarchical porous surface. The effect of the above surface treatments on the surface roughness, wettability, electrochemical corrosion behavior, apatite forming ability and cellular behavior of UFG Ti were systematically investigated with the coarse-grained Ti as control. Results show that UFG-Ti with surface modification had no pitting corrosion and presented low corrosion rate in simulated body fluids (SBF). The hierarchical porous surface yielded by surface modification enhanced the ability of UFG Ti to form a complete apatite layer when soaked in SBF and promoted osteoblast-like cells attachment and proliferation in vitro, which promises to have a significant impact on increasing bone-bonding ability and reducing healing time when implanted due to faster tissue integration.

© 2011 Elsevier B.V. All rights reserved.

1. Introduction

Till now, titanium is still the most commonly used biometal to manufacture orthopaedic prostheses on account of its excellent corrosion resistance and biocompatibility. However, the mechanical strength of commercially pure titanium (CP titanium) is relatively low compared to other metals used in biomedical devices which confined its application under heavy load conditions [1]. Either alloying or secondary processing could enhance its mechanical performance, whereas alloying adds the risk of being potentially toxic. Recently, Valiev et al. [2–4] reported that nanostructured CP titanium fabricated by severe plastic deformation (SPD) processing could improve the mechanical properties and biological response of CP titanium. Others found that ultrafine-grained titanium has improved strength and high cycle fatigue limit [5,6]. Thus, ultrafine-grained titanium (UFG Ti) is a unique biomaterial candidate due to its excellent combination of mechanical properties and cytocompatibility.

Although UFG Ti shows better biological performance than its course-grained counterparts [3,7,8], it is still bioinert by nature and cannot form a bioactive bond with the living bone if implanted in a bony site. For clinical applications, both qualified substrate and excellent surface character are necessary for implants to ensure its osseointegration and long-term functional interface between the implant and the bone bed. And especially, surface bioactivity is highly expected for an implant to promote the cell adhesion and accelerate the formation of new bone. Therefore surface modification was employed and numerous methods such as grit blasting [9], chemical etching [10,11], micro-arc oxidation [12,13] and plasma spraying [14] were developed. These methods put emphases either on surface structure and topography or surface chemistry, while in vitro and in vivo results show both of them are paramount to improve surface bioactivity and achieve osseointegration and long-term stability [9,15–18]. To best of our knowledge, only two studies have been reported to endow ultrafine-grained titanium with bioactivity either by micro-arc oxidation [13] or by grit-blasting [19], while the former only reported apatite forming behavior of the surface modified layer and the later one was about the cell behavior with respect to biocompatibility. Meanwhile, TiO_2 film fabricated by magnetron sputtering on ultrafine-grained titanium was reported to improve the blood compatibility [20].

* Corresponding author at: Department of Advanced Materials and Nanotechnology, College of Engineering, Peking University, Beijing 100871 China.
Tel.: +86 10 6276 7411; fax: +86 10 6276 7411.
** Co-corresponding author.
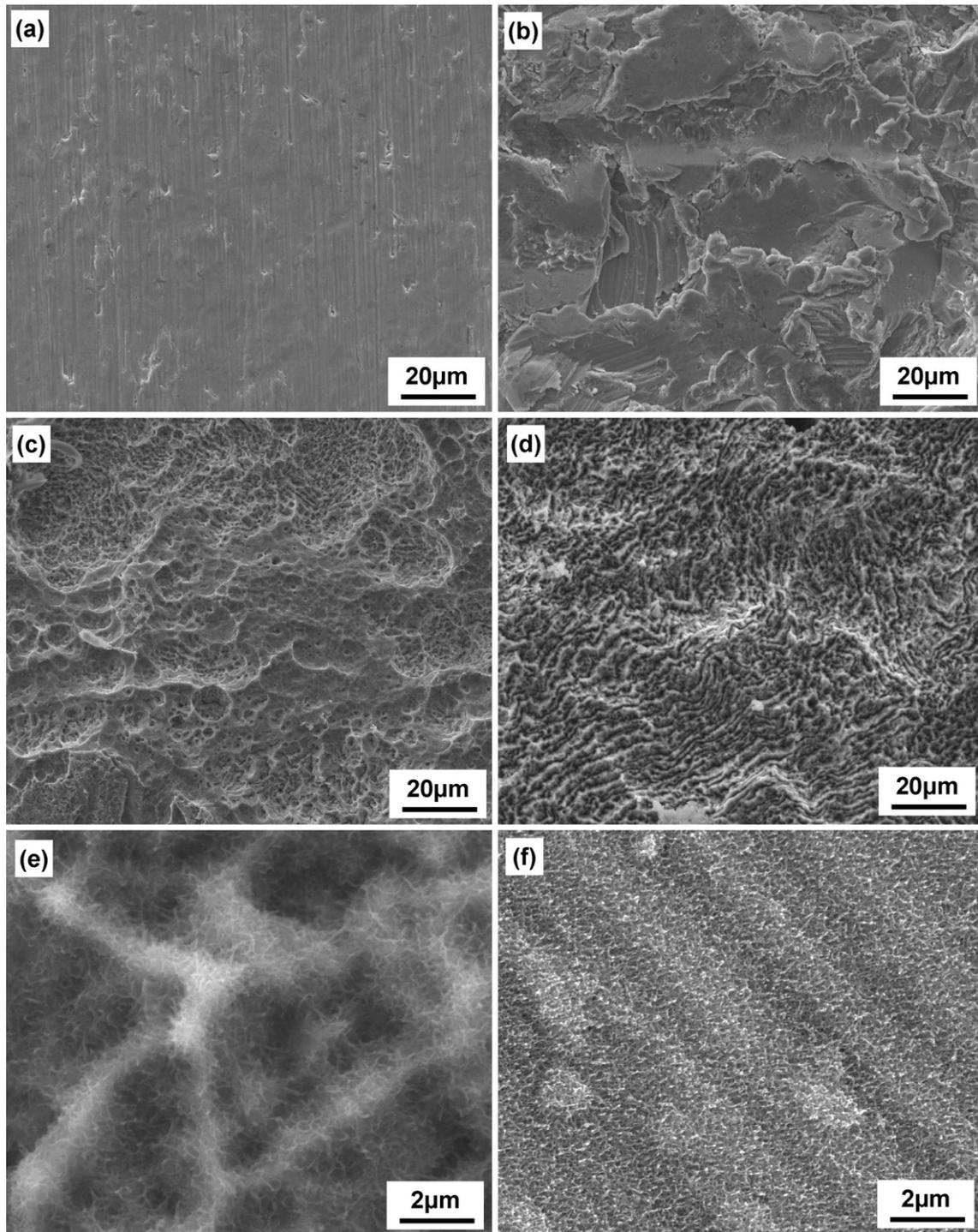E-mail address: yfzheng@pku.edu.cn (Y.F. Zheng).

Fig. 1. SEM surface morphologies with different surface modification: (a) ground UFG Ti, (b) sandblasted UFG Ti, (c) sandblasted UFG Ti with acid etching, (d) sandblasted UFG Ti with acid and alkaline etching, (e) high magnification of (d), and (f) CG Ti with alkali plus heat treatment.

In the present investigation, a new hierarchical porous surface with suitable surface topography and chemistry for implantation was fabricated on the UFG Ti substrates in the first instance with the aim of providing a promising biometal with sufficient mechanical properties of substrate and good biocompatibility of surface. The effect of the hierarchical porous surface on the in vitro biocompatibility of UFG Ti, such as apatite forming ability, cellular performance and corrosion behavior was studied.

2. Materials and methods

2.1. Materials

Ultrafine-grained Ti (dubbed UFG Ti) was prepared by equal channel angular pressing (ECAP) technique from commercial coarse-grained pure titanium (dubbed CG Ti) discs (both provided by Ufa State Aviation Technical University) with subsequent anneal in vacuum at a temperature of 300 °C for 30 min. It has equiaxed
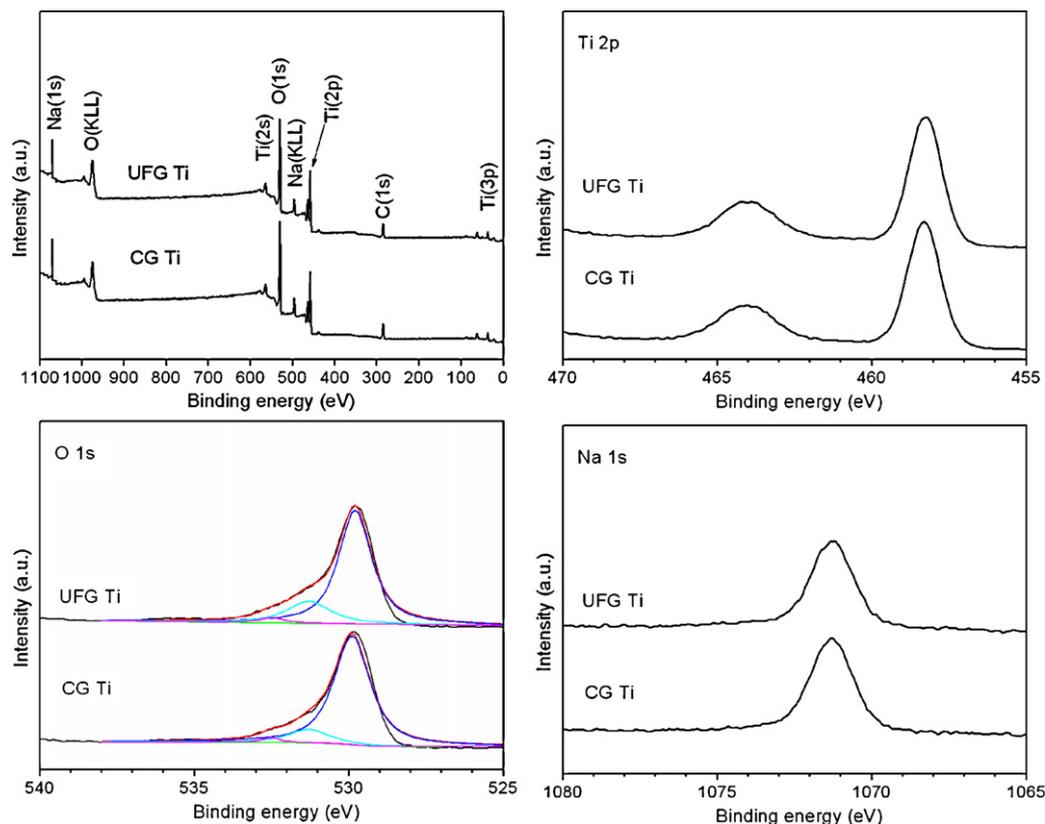
Fig. 2. XPS survey spectrum, Ti 2p, O 1s, Na 1s spectra of UFG Ti and CG Ti after three-step treatment.

grains with a mean grain size of about 280 nm [21]. The UFG Ti were ground with SiC paper up to 2000 grit, and half of them were surface modified as following procedures (dubbed UFG Ti-SM): firstly grit blasted by 60 grit corundum particles at the pressure of 0.5 MPa, then cleaned ultrasonically in acetone, ethanol and distilled water in turn for 10 min, subsequently etched in 40% HCl at 100 °C for 10 min, finally immersed in 1.5 M NaOH solution at 60 °C for 24 h. At last, all the samples were rinsed in distilled water and dried at 40 °C in a dryer.

2.2. Apatite forming ability tests

The apatite forming ability of CG Ti, UFG Ti and UFG Ti-SM was evaluated by soaking in simulated body fluid (SBF) with pH value 7.4 proposed by Kokubo without organic species [22]. The ion concentrations are as follows: Na^+ 142.0, K^+ 5.0, Mg^{2+} 1.5, Ca^{2+} 2.5, HCO_3^- 4.2, Cl^- 147.8, HPO_4^{2-} 1.0, SO_4^{2-} 0.5 mM, which is nearly equal to those of human blood plasma except HCO_3^- being 27.0 mM. Each sample was incubated in 20 ml of SBF in a Teflon-sealed bottle for 4 days at 37 °C with solution changed every other day. After the above soaking, the samples were rinsed in distilled water and dried at 40 °C in a dryer.

2.3. Cell experiment

Cell adhesion and proliferation tests were performed with osteoblast-like cell line MG63 (CRL1427, ATCC, USA). Before performing these assays, the cells were cultured in MEM medium (Invitrogen) supplemented with 10% of fetal calf serum and 1% penicillin/streptomycin at 37 °C in a humidified atmosphere of 5% CO_2 in air. MG63 cells were seeded onto the CG Ti, UFG Ti, UFG Ti-SM in 24-well culture plates at a density of 5×10^4 cells well^{-1} for direct cell adhesion observation. After 4 h incubation, the culture

media were removed and specimens were fixed with 2.5% glutaraldehyde solution for 1 hour at room temperature and rinsed 3 times with phosphate buffer solution (PBS, pH 7.4), followed by dehydration in a gradient ethanol/distilled water mixture (50%, 60%, 70%, 80%, 90%, 100%) for 10 min and dried in air. Samples were sputter coated with gold for cell morphology observation using SEM.

For the evaluation of cell attachment, cells were cultured for 4 h and 24 h in 24-well culture plates at an initial seeding density of 5×10^4 cells well^{-1}. After trypsinization of the attached cells, cell numbers were counted using a hemocytometer. Cell proliferation was determined using 3-(4,5-dimethylthiazol-2-yl)-2-5-diphenyltetrazolium bromide (MTT; Sigma) assay by a colorimetric assay. Cells were seeded at a concentration of 5×10^4 cells well^{-1} onto the sample in MEM under standard cell-culture condition described above. The control groups involved the use of MEM medium as negative control and MEM medium with 10% dimethylsulfoxide as positive control. The cells were harvested for the MTT assay at 3, 7 and 9 days. At each stage, 60 μl/well of MTT were added to each well and the cells were incubated for 4 h at 37 °C. Afterwards, 600 μl formazan solubilization solution (10% SDS in 0.01 M HCl) was added to each well for 12 h in the incubator in a humidified atmosphere. The spectrophotometrical absorbance of the samples was measured by microplate reader (Bio-RAD680) at 570 nm with a reference wavelength of 630 nm.

Table 1
Surface roughness and contact angle of CG Ti, UFG Ti and UFG Ti-SM.

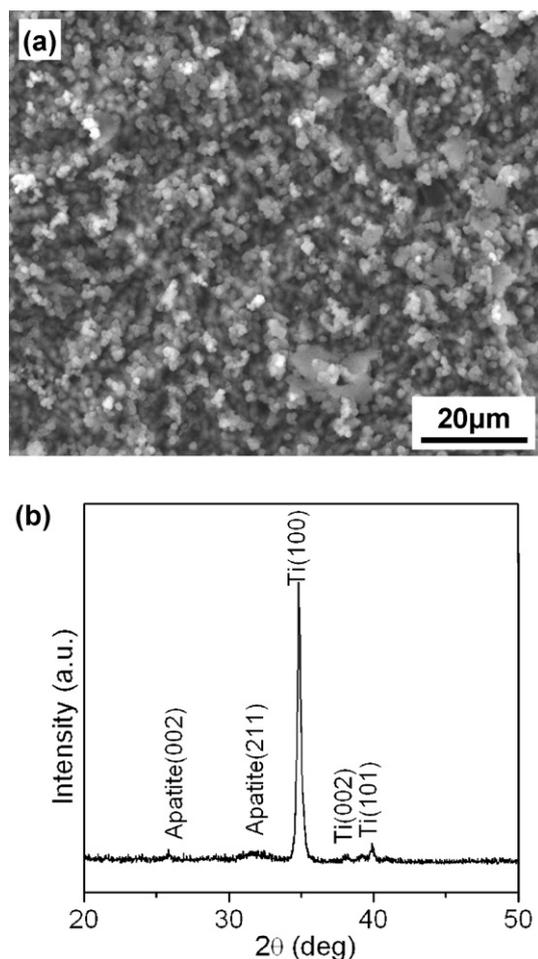| Sample	R_a (μm)	Contact angle (°)
CG Ti	0.114 ± 0.012	90.5 ± 3.6
UFG Ti	0.116 ± 0.007	81.8 ± 3.5
UFG Ti-SM	2.439 ± 0.055	40.2 ± 4.8

Fig. 3. SEM morphologies (a) and XRD profiles (b) of UFG Ti-SM soaked in SBF for 4 days.

2.4. Corrosion behavior

The electrochemical corrosion measurements were performed in SBF using an electrochemical workstation (CHI600C, China) at room temperature. The sample was set as a working electrode, a platinum electrode acting as an auxiliary electrode and the reference electrode a saturated calomel electrode (SCE). The open circuit potential measurement was maintained up to 7200 s. Potentiodynamic polarization curves were then measured from −800 mV (vs. SCE) to 2500 mV (vs. SCE) with a scan rate of 1 mV/s.

2.5. Materials characterization

Before and after experimental tests, the surface morphology and composition of the samples were assessed by environmental scanning electron microscope (ESEM, AMRAY-1910FE) and analyzed by X-ray photoelectron spectroscopy (XPS, AXIS-Ultra Instrument). Surface wettability was tested by contact angle in quintuplicate (Dataphysics Instrument, Germany).

3. Results and discussion

3.1. Surface characterization

The surface morphology of UFG Ti alloy changed significantly with different surface modification as Fig. 1 shows. The ground UFG Ti without surface treatment had a smooth surface (Fig. 1(a)). Grit

blasting produced a damaged and roughened surface (Fig. 1(b)). Subsequent acid etching in HCl solution yielded a porous surface with pores ranging from several microns to tens of microns (Fig. 1(c)). In addition, it has another benefit of eliminating the corundum particles resided during grit blasting process which has been proven to cause a contamination of implant surface and have unfavorable effects on its bone integration [23]. Hierarchical porous surface was fabricated by above treatments with following alkaline etching in NaOH solution (Fig. 1(d and e)). The big pores were tens of microns in size, among which middle-size pores about several microns with small pores in nano-scale inside were uniformly distributed. However, surface modification like alkaline plus heat treatment was usually employed onto titanium to produce a bioactive surface layer [11,24]. Titanium was treated in 5 M NaOH solution at 60 °C for 24 h then heat treated at 600 °C for 1 h. It produced a porous network surface as Fig. 1(f) shows, which is completely different from the hierarchical porous surface fabricated by three-step treatment in this study (Fig. 1(e)). XPS analysis (Fig. 2) was conducted to elucidate the chemical compositions of the modified surface layer. The main components of the outmost surface layer of UFG Ti after above three-step treatment was Ti, O and Na, which is consistent with that of CG Ti with the same treatment. Na was found to be in its ionic form Na^+ and Ti is in its four-valent state, as confirmed by the Na 1 s signal at 1071.3 eV and Ti 2p signal at 457.8 eV (Fig. 2). A three-component O 1s band that can be attributed to a combination of O^{2-}, OH^- and absorbed H_2O evidenced by the corresponding O 1s peaks at 529.7, 531.6 and 533.0 eV, respectively [25]. The combined binding energy results
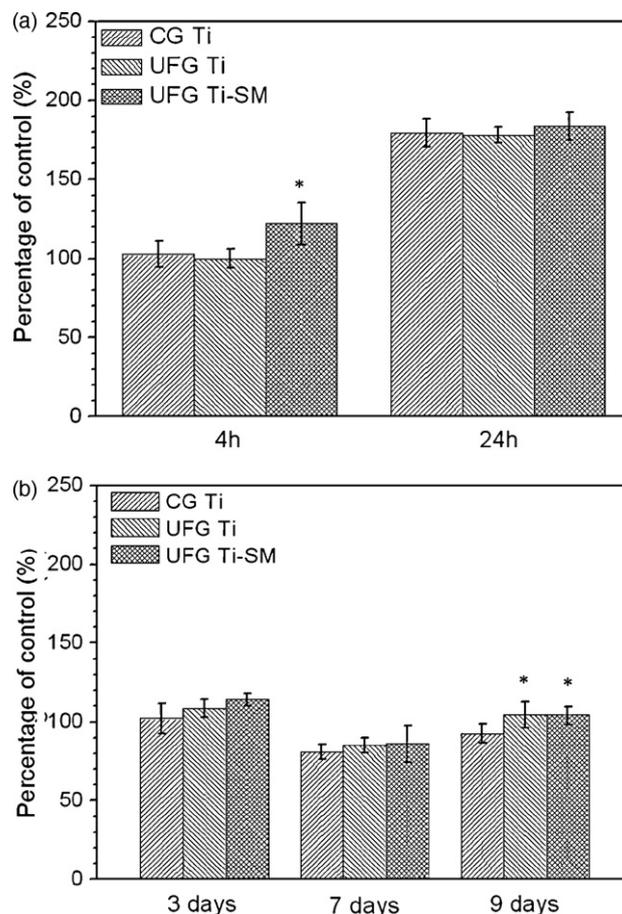

Fig. 4. Cell attachment (a) and proliferation (b) of MG 63 cultured on CG Ti, UFG Ti, and UFG Ti-SM. Columns marked with the *, represent significant difference ($P < 0.05$) for UFG Ti and UFG Ti-SM groups compared to the CG Ti group.
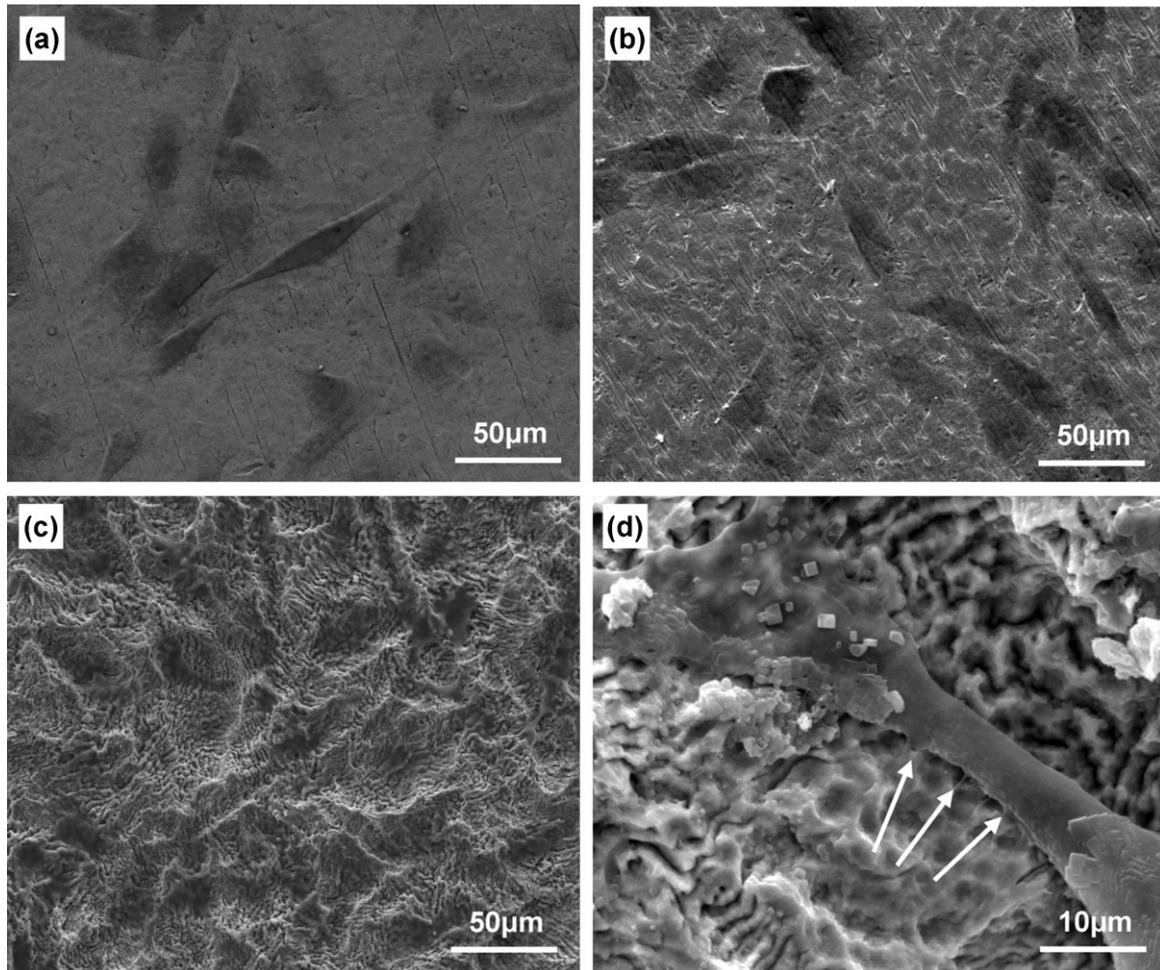
Fig. 5. SEM morphologies of MG63 cells cultured on (a) CG Ti, (b) UFG Ti, (c) UFG Ti-SM, and (d) high magnification of (c).

of Ti, O, Na suggest that sodium titanate formed during alkaline etching on the surface of UFG Ti and CG Ti. Surface roughness results (Table 1) demonstrate that the arithmetic average roughness (R_a) of UFG Ti-SM is $2.439 \pm 0.055\,\mu m$, which is over twenty times higher than that of machined UFG Ti being $0.116 \pm 0.007\,\mu m$ and is higher than the grit-blasted UFG Ti in Ref. [19] ($1.48 \pm 0.18\,\mu m$) by using hydroxyapatite particles.

3.2. In vitro biocompatibility of UFG Ti-SM

The in vitro biocompatibility of UFG Ti-SM was analyzed from aspects of apatite forming ability, cellular performance and corrosion behavior with UFG Ti and CG Ti as control. The capacity of apatite formation in SBF has been widely used to assess the bioactivity of biomaterials. Such simple test in vitro has been reported to be consistent with the in vivo test. Thus, the bioactivity of three kinds of samples was evaluated in SBF. SEM results in Fig. 3(a) and XRD results in Fig. 3(b) show that a complete and thick apatite layer formed on the surface of UFG Ti-SM when soaked in SBF for 4 days, which means the hierarchical porous surface of UFG Ti-SM fabricated by three-step treatment is highly bioactive. Meanwhile, both machined CG Ti and UFG Ti surface had only a few calcium phosphate particles deposited within 4 days soaking (pictures not shown). The increased apatite forming ability of UFG Ti-SM was attributed to the outmost sodium titanate layer and the hierarchical porous surface. During the SBF soaking, sodium ions released from the substrate via exchange with the H_3O^+ ions in the SBF form-

ing the Ti–OH groups on the titanium surfaces. These Ti–OH groups induced the apatite nucleation [11]. The release of sodium ions also accelerated apatite nucleation by increasing the OH^- concentration. The hierarchical porous surface on UFG Ti-SM increased the specific surface area compared with the smooth surface of UFG Ti, which increased the amount of OH^- groups. Meanwhile, the surface area exposed to the SBF solution was also increased and it promoted the incorporation of calcium and phosphate ions, therefore accelerated the formation of apatite. The increased surface bioactivity and acceleration in the rate of apatite formation is significant, as it should allow for earlier load bearing of prostheses following implantation.

Fig. 4 shows the results of cell behavior for all the samples after cultured for different time. It can be seen that all samples shows high cell attachment and proliferation rate. Cell attachment test results in Fig. 4(a) demonstrate that the number of cells attached to UFG Ti-SM surfaces is highest among three kinds of samples at early stage of cell culture. The cell proliferation results in Fig. 4(b) indicate that all surfaces have good cytocompatibility with a proliferation ratio over 80% of control at all culture time. The UFG Ti and UFG Ti-SM surfaces show a significant higher proliferation ratio than CG Ti surface at 9 days culture. Fig. 5 shows the SEM morphologies of cells after culture for 4 h on CG Ti, UFG Ti and UFG Ti-SM surfaces. All surfaces show health cell morphology after 4 h culture. Differently, MG63 cells closely attached to the surface of UFG Ti-SM sample with pseudopodia protruding and anchoring the surrounding substrates as arrows in Fig. 5(d) mark thus strongly
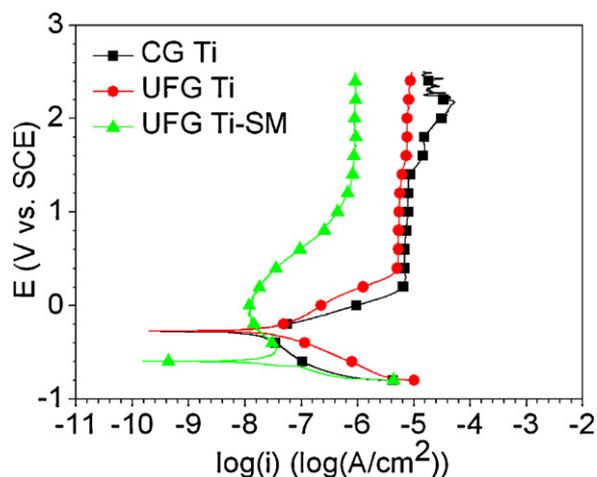
Fig. 6. Potentiodynamic polarization curves of CG Ti, UFG Ti and UFG Ti-SM.

suggesting quite adhesion capabilities. Since surface of titanium implants must allow an optimal cell and tissue adhesion to induce a satisfactory early and late bone anchorage, it seems reasonable to assume that the hierarchical porous surface is a promising surface topography.

Although a mass of in vitro electrochemical tests have confirmed that the stable and tightly adherent passive titanium oxide layer of CP titanium and different types of titanium alloy naturally formed in air is highly corrosion-resistant in simulated body fluid [26,27], such oxide layer is usually damaged or rebuilt in order to achieve surface bioactivity during surface modification, which would probably impair the corrosion resistance. Thus, it is necessary to evaluate the effect of surface treatment on the corrosion resistance of UFG Ti. In this study, hierarchical porous surface was fabricated. Potential concern about the pores to suffer from localized corrosion such as pitting and crevice corrosion was raised. The potentiodynamic polarization behaviors of UFG Ti before and after surface modification are depicted by polarization curves in Fig. 6. Values of corrosion current density (i_{corr}), corrosion potential (E_{corr}), passive current density (i_{pass}) extracted from the curves are shown in Table 2. One can see that CG Ti and UFG Ti shows similar corrosion behavior. The i_{corr} of UFG Ti-SM was 0.0231 nA/cm^2 comparable to that of UFG Ti being 0.0259 nA/cm^2. The i_{pass} of UFG Ti-SM was almost one order of magnitude lower than UFG Ti. Especially, the anodic current density of UFG Ti-SM was decreased significantly compared to that of CG Ti and UFG Ti when the potential is higher than 0 mV (SCE), which suggests very low level of corrosion rate. Meanwhile, no pitting corrosion of UFG Ti-SM was observed. However, the E_{corr} of UFG Ti-SM was decreased from -274 mV (SCE) to -598 mV (SCE), which means increased corrosion tendency. It relates to the hydrolysis tendency of outmost sodium titanate layer. Since the corrosion current was rather low compared to that of CG Ti and UFG Ti, it would be still safe when implanted. Further research needs to be done.

Above results of accelerating apatite formation and promoting MG63 cells adhesion and proliferation as well as low corrosion rate in SBF confirmed the enhanced biocompatibility of UFG Ti with hierarchical porous surface. The enhancement is not only attributed to its topography but also its surface chemistry. On the one hand, the surface roughness (R_a) of UFG Ti-SM is more than twenty times that of UFG Ti. Generally, increased surface roughness enhances bone integration of implants [28]. High surface roughness and three-dimensional micro- and nano-structured surface pores increased the specific surface area, which would enhance the surface reactivity with the surrounding ions, amino acids and proteins, which determine the initial adsorption of calcium and phosphate ions as well as cellular events at the cell-material interface. On the other hand, the water contact angle of UFG Ti-SM (Table 1) is about $40.2 \pm 4.8°$ and UFG Ti being $81.8 \pm 3.5°$, which means UFG Ti-SM sample surface is much more hydrophilic than UFG Ti surface. It is reported that hydrophilic surfaces (20–40° water contact angle) promoted cell attachment [29].

It is noteworthy that the three-step treatment of grit blasting, acid etching and alkaline treatment was used in this study instead of commonly used alkaline with heat treatment [11,24]. Heat treatment at high temperature or other treatment which would cause sharp increase of the substrate temperature should be avoided to protect the ultrafine-grained structure for the UFG Ti or other ultrafine-grained material matrix. The growth of grain size impairs the mechanical properties of ultrafine-grained materials. Generally, titanium implants with a microrough surface achieve faster bone integration, a higher percentage of bone-implant contact and higher removal torque values when compared with titanium implants with a polished or machined surface [30]. Thus, the surface modified UFG Ti with a hierarchical porous bioactive surface in this study together with previously reported superior mechanical properties is potentially be one of the best choices of biometals for applications in bone implantology.

4. Conclusions

In summary, the hierarchical porous surface layer with increased surface roughness and wettability enhanced the in vitro surface biocompatibility of ultrafine-grained titanium, which was produced by combined grit blasting, acid etching and alkaline treatment. Such porous surface showed no pitting corrosion and presented low corrosion rate in SBF. Meanwhile, it increased the ability to form a complete apatite layer when soaked in SBF and promoted osteoblast-like cells attachment and proliferation in vitro compared to untreated ultrafine-grained and coarse-grained titanium surface, which promises to have a significant impact on increasing bone-bonding ability and reducing healing time when implanted due to faster tissue integration.

Acknowledgments

References

[1] M. Niinomi, Mechanical properties of biomedical titanium alloys, Mater. Sci. Eng. A 243 (1–2) (1998) 231–236.
[2] A.V. Sergueeva, V.V. Stolyarov, R.Z. Valiev, A.K. Mukherjee, Advanced mechanical properties of pure titanium with ultrafine grained structure, Scr. Mater. 45 (7) (2001) 747–752.
[3] R.Z. Valiev, I.P. Semenova, E. Jakushina, V.V. Latysh, H. Rack, T.C. Lowe, J. Petruželka, L. Dluhoš, D. Hrušák, J. Sochová, Nanostructured SPD processed titanium for medical implants, Mater. Sci. Forum 584/586 (2008) 49–54.
[4] V.S. Zhernakov, V.V. Latysh, V.V. Stolyarov, A.I. Zharikov, R.Z. Valiev, The developing of nanostructured SPD Ti for structural use, Scr. Mater. 44 (8–9) (2001) 1771–1774.
[5] W.J. Kim, C.Y. Hyun, H.K. Kim, Fatigue strength of ultrafine-grained pure Ti after severe plastic deformation, Scr. Mater. 54 (10) (2006) 1745–1750.

Table 2
Results of electrochemical parameters.

Sample	E_{corr} (mV (SCE))	i_{corr} (nA/cm^2)	i_{pass} (nA/cm^2)
CG Ti	-278	0.0326	30.9
UFG Ti	-274	0.0259	42.8
UFG Ti-SM	-598	0.0231	5.64

[6] X.C. Zhao, W.J. Fu, X.R. Yang, T.G. Langdon, Microstructure and properties of pure titanium processed by equal-channel angular pressing at room temperature, Scr. Mater. 59 (5) (2008) 542–545.

[7] T.N. Kim, B.C. Lee, W.S. Kim, K. Smetana, J.K. Park, B.B. Panigrahi, In vitro biocompatibility of equal channel angular processed (ECAP) titanium, Biomed. Mater. 2 (2007) S117–S120.

[8] R.Z. Valiev, I.P. Semenova, V.V. Latysh, H. Rack, T.C. Lowe, J. Petruzelka, L. Dluhos, D. Hrusak, J. Sochova, Nanostructured titanium for biomedical applications, Adv. Eng. Mater. 10 (8) (2008) B15–B17.

[9] A. Wennerberg, T. Albrektsson, C. Johansson, B. Andersson, Experimental study of turned and grit-blasted screw-shaped implants with special emphasis on effects of blasting material and surface topography, Biomaterials 17 (1) (1996) 15–22.

[10] H.B. Wen, Q. Liu, J.R. De Wijn, K. De Groot, F.Z. Cui, Preparation of bioactive microporous titanium surface by a new two-step chemical treatment, J. Mater. Sci. Mater. Med. 9 (1998) 121–128.

[11] H.M. Kim, F. Miyaji, T. Kokubo, Effect of heat treatment on apatite-forming ability of Ti metal induced by alkali treatment, J. Mater. Sci. Mater. Med. 8 (1997) 341–347.

[12] H.T. Chen, C.H. Hsiao, H.Y. Long, C.J. Chung, C.H. Tang, K.C. Chen, J.L. He, Micro-arc oxidation of beta-titanium alloy: structural characterization and osteoblast compatibility, Surf. Coat. Tech. 204 (6–7) (2009) 1126–1131.

[13] Z.Q. Yao, Y. Ivanisenko, T. Diemant, A. Caron, A. Chuvilin, J.Z. Jiang, R.Z. Valiev, M. Qi, Synthesis and properties of hydroxyapatite-containing porous titania coating on ultrafine-grained titanium by micro-arc oxidation, Acta Biomater. 6 (7) (2010) 2816–2825.

[14] P. Cheang, K.A. Khor, Addressing processing problems associated with plasma spraying of hydroxyapatite coatings, Biomaterials 17 (5) (1996) 537–544.

[15] A. Curtis, C. Wilkinson, Topographical control of cells, Biomaterials 18 (24) (1997) 1573–1583.

[16] M. Bigerelle, K. Anselme, B. Noel, I. Ruderman, P. Hardouin, A. Iost, Improvement in the morphology of Ti-based surfaces: a new process to increase in vitro human osteoblast response, Biomaterials 23 (7) (2002) 1563–1577.

[17] G. Giavaresi, L. Ambrosio, G.A. Battiston, U. Casellato, R. Gerbasi, M. Finia, N.N. Aldini, L. Martini, L. Rimondini, R. Giardino, Histomorphometric, ultrastructural and microhardness evaluation of the osseointegration of a nanostructured titanium oxide coating by metal-organic chemical vapour deposition: an in vivo study, Biomaterials 25 (25) (2004) 5583–5591.

[18] G. Giavaresi, M. Fini, A. Cigada, R. Chiesa, G. Rondelli, L. Rimondini, P. Torricelli, N.N. Aldini, R. Giardino, Mechanical and histomorphometric evaluations of titanium implants with different surface treatments inserted in sheep cortical bone, Biomaterials 24 (9) (2003) 1583–1594.

[19] J.W. Park, Y.J. Kim, C.H. Park, D.H. Lee, Y.G. Ko, J.H. Jang, C.S. Lee, Enhanced osteoblast response to an equal channel angular pressing-processed pure titanium substrate with microrough surface topography, Acta Biomater. 5 (8) (2009) 3272–3280.

[20] H.H. Shao, C.H. Yu, X.J. Xu, J. Wang, R. Zhai, X.J. Wang, Influence of Ti nanocrystallization on microstructure, interface bonding, surface energy and blood compatibility of surface TiO_2 films, Appl. Surf. Sci. 257 (5) (2010) 1649–1654.

[21] V.V. Stolyarov, Y.T. Zhu, I.V. Alexandrov, T.C. Lowe, R.Z. Valiev, Grain refinement and properties of pure Ti processed by warm ECAP and cold rolling, Mater. Sci. Eng. A 343 (1–2) (2003) 43–50.

[22] T. Kokubo, H. Takadama, How useful is SBF in predicting in vivo bone bioactivity? Biomaterials 27 (15) (2006) 2907–2915.

[23] M. Rüger, C. Herren, T.J. Gensior, C. Herren, M. von Walter, C. Ocklenburg, R. Marx, H.J. Erli, The removal of Al_2O_3 particles from grit-blasted titanium implant surfaces: effects on biocompatibility, osseointegration and interface strength in vivo, Acta Biomater. 6 (7) (2010) 2852–2861.

[24] H.M. Kim, F. Miyaji, T. Kokubo, S. Nishiguchi, T. Nakamura, Graded surface structure of bioactive titanium prepared by chemical treatment, J. Biomed. Mater. Res. 45 (2) (1999) 100–107.

[25] S.J. Li, R. Yang, M. Niinomi, Y.L. Hao, Y.Y. Cui, Formation and growth of calcium phosphate on the surface of oxidized Ti–29Nb–13Ta–4.6Zr alloy, Biomaterials 25 (13) (2004) 2525–2532.

[26] A. Choubey, B. Bikramjit, R. Balasubramaniam, Electrochemical behavior of Ti-based alloys in simulated human body fluid environment, Trends Biomater. Artif. Organs 18 (2) (2005) 64–72.

[27] M.F. López, A. Gutiérrez, J.A. Jiménez, In vitro corrosion behaviour of titanium alloys without vanadium, Electrochim. Acta 47 (9) (2002) 1359–1364.

[28] F. Grizon, E. Aguado, G. Hure, M.F. Basle, D. Chappard, Enhanced bone integration of implants with increased surface roughness: a long term study in the sheep, J. Dent. 30 (5–6) (2002) 195–203.

[29] K. Webb, V. Hlady, P.A. Tresco, Relative importance of surface wettability and charged functional groups on NIH 3T3 fibroblast attachment, spreading, and cytoskeletal organization, J. Biomed. Mater. Res. 41 (3) (1998) 422–430.

[30] D.M. Brunette, P. Tengvall, M. Textor, P. Thomsen, Titanium in Medicine: Material Science, Surface Science, Engineering, Biological Responses and Medical Applications, Springer, New York, 2001, pp. 878.